

Original Article

Untargeted metabolomics analysis for a strain of *Bacillus subtilis* isolated from the oral cavity

Huimin Huang^{1*}, Liping Chen^{2*}, Ziyang Nie³, Xiaofeng Zhang³, Genyun Yi³, Shengrong Wu³, Jing Wang³, Jianye Zhou¹, Zhiqiang Li¹

¹Key Laboratory of Oral Diseases, Key Lab of Stomatology of State Ethnic Affairs Commission, Lanzhou, Gansu, China; ²West China Hospital, Sichuan University, Chengdu, China; ³School of Stomatology, Lanzhou University, Lanzhou, China. *Equal contributors.

Received October 6, 2017; Accepted February 2, 2018; Epub April 15, 2018; Published April 30, 2018

Abstract: *Aim:* This study aimed to explore the possible small molecular metabolites of *B. subtilis* zh78 that can inhibit growth of cariogenic bacteria and to evaluate the prospect of *B. subtilis* zh78 in caries prevention and management. *Methods:* Cold methanol was adopted to extract the metabolites in bacteria solutions from the *B. subtilis* zh78 growth at 0 hour, 7 hours, 12 hours and 5 days, respectively. The gas chromatography was coupled with the time of flight mass spectrometry (GC-TOF-MS), which were applied to metabolomics detection. Data were analyzed and processed by using cluster analysis combined with orthogonal partial least squares discriminant analysis (OPLS-DA) and Pearson's correlation analysis. *Results:* There were a total of 15 kinds of substances (e.g. xylitol, L-glutamic acid, and L-tyrosine) produced by *B. subtilis* zh78 which were significantly correlated to growth inhibition on *Streptococcus mutans* (*S. mutans*), *Actinomyces viscosus* (*A. viscosus*), and *Lactobacillus acidophilus* (*L. acidophilus*). *Conclusion:* The findings suggest that *Bacillus subtilis* zh78 could produce 15 kinds of metabolites (e.g. xylitol, L-glutamic acid, and L-tyrosine) which might exert antibacterial effects on *S. mutans*, *L. acidophilus*, and *A. viscosus*. *B. subtilis* zh78 displayed its potential in oral probiotic application and related studies.

Keywords: *Bacillus subtilis*, metabolomics, antibacterial activity, differential metabolites

Introduction

Dental caries is one of the most prevalent infectious diseases globally, characterized by progressive tooth demineralization due to the action of bacterial acid metabolism [1, 2]. Among the numerous pathogenic bacteria, *Streptococcus mutans* (*S. mutans*), *Actinomyces viscosus* (*A. viscosus*), and *Lactobacillus acidophilus* (*L. acidophilus*) have been confirmed as the primary pathogens due to the fact that they can metabolize carbohydrates and produce organic acids that result in the demineralization of tooth enamel [3, 4]. Prevention and management of dental caries depends on the effective control of these cariogenic bacteria [5]. However, some traditional approaches (e.g. using antibiotics and mouthwashes) to control cariogenic bacteria have achieved only limited success. Novel methods such as whole bacteria replacement therapy to decrease pathogens in oral cavities should be inves-

tigated [6, 7]. It is of value to study a strain of oral indigenous bacteria to inhibit the growth of the three kinds of the pathogenic bacteria (*S. mutans*, *A. viscosus*, and *L. acidophilus*) and to exploit their related metabolites.

Bacillus subtilis (*B. subtilis*) is a rod-shaped Gram-positive facultative anaerobe widely existing in the natural environment and gastrointestinal tract of animals in enormous quantities [8]. It can utilize some substances to synthesize its own nutrients and produce functional products [9]. Therefore, it has been well-developed and applied in many fields including botany, medicine, and food technology. *B. subtilis* has been detected and isolated from the oral cavity in humans by Naidorf et al. [10-12] and its morphological and physico-chemical characteristics have also been simultaneously identified. We found a strain of *B. subtilis* and named it as *B. subtilis* zh78 in our previous study. It can inhibit the growth of the three

kinds of the pathogenic bacteria (*S. mutans*, *L. acidophilus*, and *A. viscosus*). However, its bacteriostatic components were still ambiguous [13].

With the remarkable progress in the field of metabolomics over the last decade, it is possible to rapidly and simultaneously measure thousands of metabolites from minimal amounts of samples [14]. Untargeted metabolomic methods are global in scope, with an aim to simultaneously measure metabolites, as many as possible from biological samples without bias. This method has great potential to provide insights into fundamental biological processes [14]. In this study, we adopted metabolites extracted by the cold methanol from *B. subtilis zh78* to perform bacteriostasis assay. Then, an untargeted GC-TOF-MS-based metabolomics approach was utilized to measure metabolites at each stage of *B. subtilis zh78* growth. Data were analyzed and processed by using cluster analysis, orthogonal partial least squares discriminant analysis (OPLS-DA), and Pearson's correlation analysis. This study aimed to identify the metabolites from *B. subtilis zh78* that could preliminarily inhibit the growth of *S. mutans*, *L. acidophilus*, and *A. viscosus*.

Materials and methods

Strains and growth conditions

The standard strains of *S. mutans* (ATCC 25-157), *L. acidophilus* (ATCC 4356), and *A. viscosus* (ATCC 15987) were obtained from the Stomatological Hospital of Peking University (Beijing, China) and stored at the Key Laboratory of Oral Diseases Research in Northwest University for Nationalities (Lanzhou, China). The strains were grown in BHI medium, which were purchased from Qingdao Hi Tech Park Hopebio Technology Co., Ltd (Shandong, China). The *B. subtilis zh78* was preserved in the Key Laboratory of Oral Diseases Research, Northwest University for Nationalities (Lanzhou, China), and was deposited in the Chinese Committee of Microbial Preservation and Management, the Institute of Microbiology, the Chinese Academy of science (Beijing, China). The growth medium of *B. subtilis zh78* was the selective T2 medium consisting of 10 g glucose, 10 g soybean protein peptone, 5 g beef extract, and 2 g yeast extract in sterile deion-

ized water per liter. The pH value was adjusted to 7. The solid medium contained 20 g agar per liter.

Derivatization reagent and GC-TOF-MS instrument

Bis-(trimethylsilyl)-trifluoroacetamide (BSTFA) with 1% trimethylchlorosilane (TMCS) solution were purchased from REGIS Technologies, Inc. (USA). The metabolites detection was performed using Agilent 7890A gas chromatograph system (J&W Scientific, Folsom, CA, USA) equipped with a DN-5 MS capillary column (30 m × 250- μ m inner diameter, 0.25- μ m film thickness) and mass spectrometer (LECO PEGASUS HT, LECO, USA).

Antimicrobial assays

In this section, we used metabolites extracted through the cold methanol from *B. subtilis zh78* to perform bacteriostasis assay. The bacteria solution samples of *B. subtilis zh78* growth were collected and set as the kb phase/group (0 hours), the zs phase/group (7 hours), the pt phase/group (12 hours), and the sw phase/group (5 days). After the frozen *B. subtilis zh78* was activated in T2 solid culture dish, its monoclonal colony was inoculated into T2 liquid medium for further cultivation. The bacteria liquids were then collected from the four growth phases of *B. subtilis zh78*, namely the kb phase (100 mL), the zs phase (100 mL), the pt phase (100 mL), and the sw phase (100 mL) were respectively centrifuged at 3000rpm for 5 minutes in the condition of 4°C. This centrifugation process was repeated 3 times. The centrifugal deposits were discarded at each time. All of the supernatant samples were filtered through the 0.22 μ m filter and cold methanol was added in each sample at a volume ratio of 4:1 (methanol/supernatant). The mixture was then centrifuged at 12000 rpm for 10 minutes in the condition of 4°C. Afterwards, the supernatant was collected and dried in a vacuum concentrator. Following these steps, the metabolites of *B. subtilis zh78* were extracted and obtained.

Subsequently, 10 parallel control groups were set to conduct the bacteriostatic assay. We prepared 10 culture dishes and placed 5 Oxford Cups in each culture dish. Among them, 4 of the Oxford Cups were respectively correspond-

ing to the metabolites at the kb, zs, pt, and sw growth phase of *B. subtilis zh78*, which were set as the experimental group. The remaining Oxford cup was set as the negative control group. We then prepared 3 copies of the BHI solid medium (100 mL), which were sterilized through autoclaving and then tempered to 45°C. Following that, the bacterial culture liquids (10^6 CFU/mL) of *S. mutans* (10 µL), *L. acidophilus* (10 µL), and *A. viscosus* (10 µL) were respectively mixed with them. Next, we dispensed the BHI solid medium into the culture dish and removed the Oxford cup with sterile tweezers after they became solid. Subsequently, the metabolites respectively obtained from the kb phase, zs phase, pt phase, and sw phase of *B. subtilis zh78* growth were dissolved by using sterile deionized water. They were then correspondingly dripped into each hole (200 µL/hole) in the experimental groups. BHI broth (200 µL) was added into each hole in the negative control group. After completing these steps, the culture plates were sealed and incubated at 37°C for 12-16 hours. Antimicrobial activity of the film was expressed in terms of inhibition zone. The diameter of the inhibition zone around the Oxford cup was measured 3 times with a millimeter scale. The mean values and standard deviations were recorded.

GC-TOF-MS sample processing and detection

There were a total of 24 metabolite samples collected from the four growth phases (kb, zs, pt, sw) of *B. subtilis zh78* for GC-TOF-MS analysis, among which 6 samples were at each phase/group. All of these samples were prepared following these steps: After the frozen *B. subtilis zh78* was activated in T2 solid culture plate, the monoclonal colony was inoculated into T2 liquid medium for further cultivation. Then, the bacterium solutions at four growth phases (kb, zs, pt, sw) of *B. subtilis zh78* were respectively selected and centrifuged at 3000 rpm for 5 minutes at 4°C. The centrifugation process was repeated 3 times. The precipitate was then discarded and supernatant was filtered through the 0.22 µm filter. The cold methanol (0.4 mL) was added to each sample (100 µL) and the mixture was then vortexed and centrifuged at 12000 rpm for 10 minutes in the condition of 4°C. The supernatant was dried in a vacuum concentrator. The obtained metabolites were suspended in

80 µL methoxyamination reagent (20 mg/mL in pyridine). The mixture was then incubated in the drying oven at 37°C for 2 hours. BSTFA reagent (0.1 mL) was then added to the aliquot samples. Following that, 10 µL standard mixture of fatty acid methyl esters (FAMES: 1 mg/mL C8-C16 and 0.5 mg/mL C18-C30 in chloroform) was added. The mixture was then detected using the GC-TOF-MS method. A single experimental sample was selected for preliminary experiment before the GC-TOF-MS test was formally carried out, which could not only guarantee the quality of samples and the stability of the instrument platform but also be beneficial in exploring the optimum methods for metabolite extraction and detection.

Statistical analysis

The software SPSS17.0 was adopted to analyze the data about the diameter of bacteriostatic circle. GC-TOF-MS analysis was performed using the software of Chroma TOF4.3X (LECO) combined with the LECO-Fiehn Rtx5 database. In this study, full similarity was set as 1000. Similarity greater than 700 indicated the identification results were credible; similarity less than 200 denoted the compound was considered as an “analyte”; similarity between 200 and 700 indicated the annotation of the analyte was regarded as putative. In addition, to simulate the missing raw data, the method of half-minimum numerical simulation was applied. The data were analyzed by using the area normalization method and noise was removed by the interquartile range method through filtering the data. Thereafter, the normalized data was imported into the software package of SIMCA-P+13.0 (Umetrics, Umea, Sweden) and R Programming Language package for cluster analysis and OPLS-DA. Based on the criteria [a variable importance in the projection (VIP) value greater than 1 and a *P* value of Student's *t* test less than 0.05], different metabolites were selected. Pearson's correlation analysis was performed to measure the correlation between the determined different metabolites and the diameter of bacteriostatic circle.

Results

The results of bacteriostatic test

The results of the bacteriostasis experiment are shown in [Figure S1](#). In the bacteria culture plates (*A. viscosus*, *L. acidophilus*, and *S.*

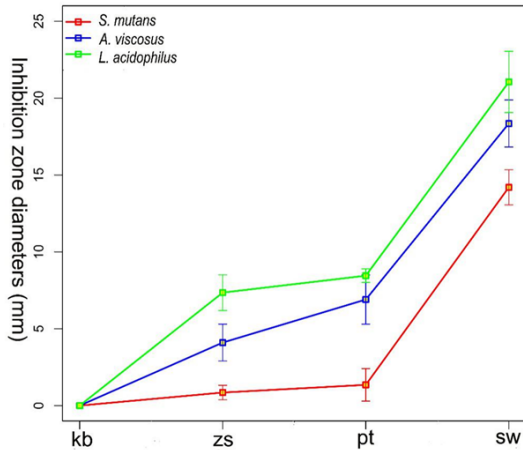


Figure 1. The Line chart showing the diameter of the bacteriostatic ring of metabolite of *Bacillus subtilis* on *S. mutans* (red line), *A. viscosus* (blue line), and *L. acidophilus* (green line) at different growth stages.

mutans), there were bacteriostatic zones around each hole in which the metabolites at different growth phases (zs, pt, and sw) were added. The inhibition zone around the pore of the metabolites at sw stage was most obvious (Figure S1). No bacteriostatic rings were found around the pores of the metabolites at kb phase of *B. subtilis zh78* and the pores of the BHI liquid medium. In the culture plate of *S. mutans*, the diameters of bacteriostatic rings were 0.85 mm-zs, 1.35 mm-pt, and 14.2 mm-sw, respectively. In the culture plate of *A. viscosus*, corresponding values for diameters were 4.1 mm-zs, 6.9 mm-pt, and 18.35 mm-sw, respectively. The corresponding values of diameters of 7.35 mm-zs, 8.45 mm-pt, and 21.05 mm-sw were measured from the culture plate of *L. acidophilus*. The diameter of inhibitory zone at sw phase was significantly greater than that of either at zs phase or at pt phase (Figure 1) which suggested that the antimicrobial activity of the metabolites at the sw phase of *B. subtilis zh78* was much stronger than at the other phases.

Statistical discrimination among the metabolites at different growth stages of B. subtilis zh78

After 24 metabolite samples were separated and detected through GC-TOF-MS, the chromatogram was obtained. There were a total of 1280 ion peaks identified and 994 metabolites remained after removing noise based on

the interquartile ranges method. The majority of these peaks were identified as endogenous metabolites, according to the LECO/Fiehn Metabolomics Library. These metabolites included fatty acids, amino acids, carbohydrates, organic acids, inorganic acids, and pyrimidines. Then, cluster analysis was performed. The cluster analysis chart (Figure S2) demonstrated that each sample could be clearly divided and the metabolites of *B. subtilis zh78* were related to its growth phases. The data expressed obvious taxonomic characteristics and no abnormal sample was rejected, which deserves further analysis.

Subsequently, a supervised OPLS-DA was applied to highlight the differences among the groups. By using one predictive and one orthogonal component, the loading plots based on OPLS-DA were constructed between the sw group and kb group (Figure 2A), between the pt group and kb group (Figure 2B), between the zs group and kb group (Figure 2C), and between the sw group and the other groups (Figure 2D), respectively (sw-kb groups: $R^2X = 0.73$, $R^2Y = 0.996$, $Q^2 = 0.987$; pt-kb groups: $R^2X = 0.716$, $R^2Y = 0.998$, $Q^2 = 0.991$; zs-kb groups: $R^2X = 0.626$, $R^2Y = 0.998$, $Q^2 = 0.984$; sw-other groups: $R^2X = 0.566$, $R^2Y = 0.98$, $Q^2 = 0.975$). Through these models, clear separation was generated between the sw and kb groups, between the pt and kb groups, between the zs and kb groups, and between the sw and remaining three groups. These values indicated that a majority of the variations in the statistical data were attributable to the above-mentioned separation between groups.

The values from the OPLS-DA model in our analysis were subsequently applied to identify the different metabolites between the sw and the kb groups, between the pt and the kb groups, between the zs and the kb groups, and between the sw and the remaining three groups. According to the criteria (the variable importance in the projection value greater than 1 and the *P* value of Student's *t* test less than 0.05), some metabolites that were significantly altered between the sw and the kb groups, between the pt and the kb groups, between the zs and the kb groups, and between the sw and the remaining three groups were identified. Following that, different metabolites between the sw and the kb groups,

Microbial metabolomics

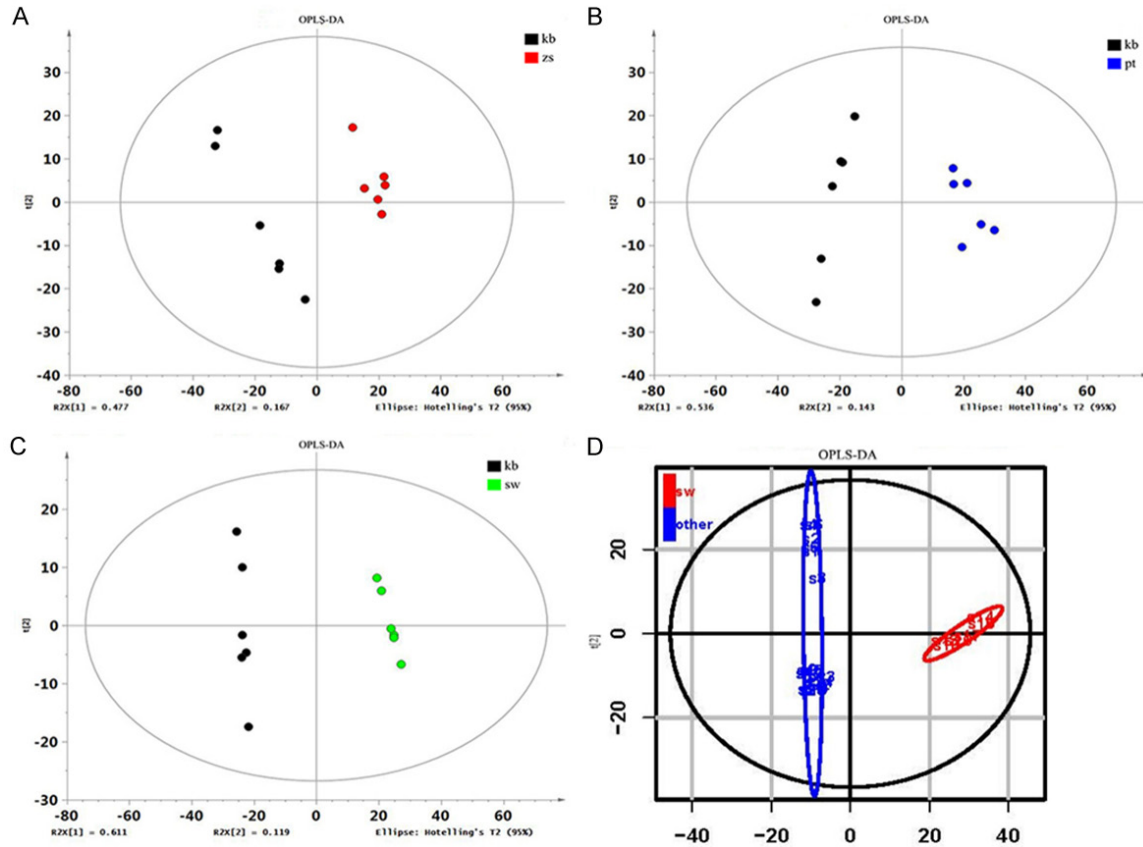


Figure 2. OPLS-DA scores plot was performed to show a clearer discrimination between zs and kb groups (A), pt and kb groups (B), sw and kb groups (C), sw and remaining three groups (D) individually of *B. subtilis* zh78. Black refers to kb group, red refers to zs group, blue refers to pt group, green refers to sw group in (A-C); red refers to sw group, blue refers to the remaining three group in (D).

between the pt and the kb groups, and between the zs and kb groups were compared together. As is shown in the Venn diagram (Figure 3), 98 different metabolites more commonly appeared in the zs, the pt, and the sw groups compared with the kb group. A total of 50 different metabolites only occurred in the sw group but not in the remaining three groups. Those 98 different metabolites and 50 unique different metabolites were analyzed through the diameter of the bacteriostatic circle by using Pearson's correlation analysis. The different metabolite with its correlation coefficient (r) closer to 1 and P value less than 0.05 were considered as having a strong correlation with bacteriostasis. The results showed that a total of 27 metabolites were significantly related to the diameter of *S. mutans* inhibitory ring; 23 metabolites were associated with the diameter of *L. acidophilus* inhibitory ring; 25 metabolites were related to the diameter of *A. viscosus* inhibitory ring. According to the literature re-

view, 15 compounds that might have bacteriostatic activity are listed in Tables 1 and 2, among which 10 substances were commonly produced at the zs, the pt, and the sw growth phases (Table 1). The other 5 substances were only produced at the sw growth phase (Table 2). The fold change (FC) in abundance was used to indicate the level of change in specific biomarkers.

Discussion

This study aimed to explore small molecular metabolites of *B. subtilis* zh78, which might have bacteriostatic property. First, we adopted cold methanol to extract the metabolites of *B. subtilis* zh78 from each growth cycle. Then, the metabolites were concentrated and were utilized for experiments to test if they had bacteriostatic effects on the three types of bacteria (*S. mutans*, *L. acidophilus*, and *A. viscosus*). The results showed that the antibacterial

Microbial metabolomics

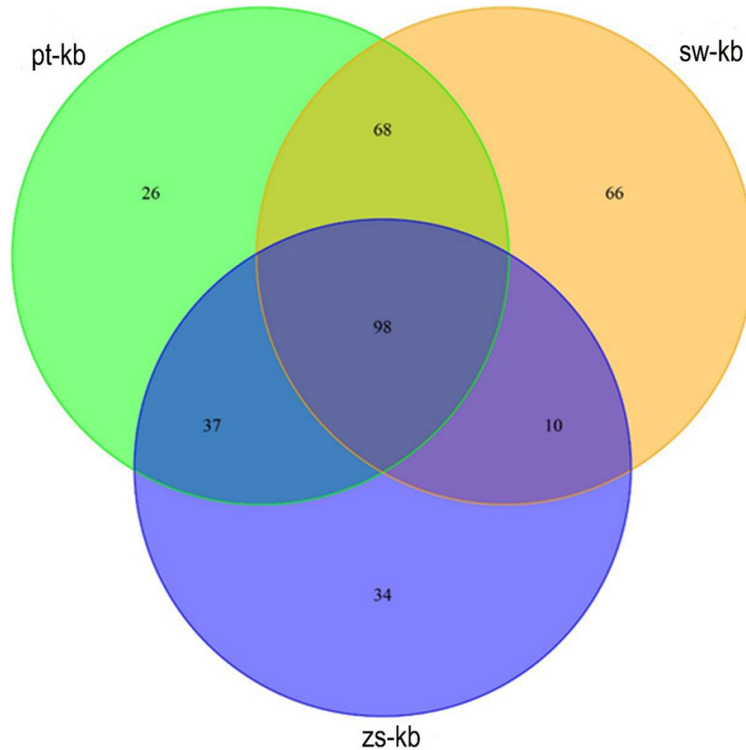


Figure 3. Venn maps of differential metabolites sw-kb (topright), pt-kb (topleft), zs-kb (lower).

effects of metabolites on each group gradually became obvious with the extension of the growth cycle. The most notable effect of metabolite was shown at the sw phase and the diameter of its inhibition zone reached 14.2, 21.05 and 18.35 mm respectively. The results fully demonstrate that metabolites of *B. subtilis zh78* could be extracted through the methanol and that using the metabolomics approach to find antibacterial substances is feasible.

Second, we used the approach of untargeted GC-TOF-MS-based metabolomics to identify altered metabolites. The results from OPLS-DA showed that the metabolites of *B. subtilis zh78* at the kb phase, the zs phase, the pt phase, and the sw phase were significantly different. Considering its antibacterial effects, *B. subtilis zh78* might produce various antibacterial substances at the different growth stages. While some of the antimicrobial substances were commonly produced at the zs, the pt, and the sw phases, some of the inhibitory substances were only produced at the sw phase. These substances might have different inhibitory ability. According to Pearson's correlation analysis

is between the different metabolites and the diameter of bacteriostatic zone, it was found that a total of 27 metabolites produced by *B. subtilis zh78* were significantly associated with its antibacterial effects on *S. mutans*; a total of 23 metabolites were related to its antibacterial effects on *L. acidophilus*; 25 of metabolites were correlated to its antibacterial effects on *A. viscosus*. The metabolites listed in **Table 1** commonly appeared at the zs, the pt, and the sw growth phase of *B. subtilis zh78* and their levels gradually increased with their growth cycle. The metabolites displayed in **Table 2** were only generated at the sw growth phase of *B. subtilis zh78*. Bactericidal functions of some metabolites have not yet been reported in previous literature. However, the bactericidal functions of some compounds

(e.g. xylose, xylitol, tartronic acid, phenylacetic acid, phenyllactic acid, phenylpyruvate, glycolic acid, L-malic acid, D-tagatose, glutaraldehyde, L-tryptophan, spermidine, xanthine, L-glutamic acid, and L-tyrosine) have been demonstrated in previous studies.

Xylitol is widely used in chewing gum due to the fact that it possesses both noncariogenic and cariostatic properties [15]. It has been demonstrated by Beenken that xylitol possesses antibacterial properties and can prevent biofilm formation [16]. It was illustrated by Reiner [17] that the nonspecific fructose phosphotransferase system in *S. mutans* could transfer xylitol to intracellular and convert it into phosphorylated metabolites, which could inhibit the growth of *S. mutans*. It was found by Hrimech [18] that xylitol could interfere with synthesis and expression of the heat shock protein 70 and the heat shock protein 60 in *S. mutans*, thus affecting its growth. The studies from S. Derling and Ly KA also have shown that xylitol could inhibit the growth of *S. mutans* [19, 20]. In addition, studies from Guo [21] and Thabuis [22] have demonstrated that xylitol

Microbial metabolomics

Table 1. Metabolites at the zs, pt, and sw phases related to the diameter of inhibitory ring

Metabolites	<i>r</i> (<i>S. mutans</i> / <i>A. viscosus</i> / <i>L. acidophilus</i>)	<i>P</i> (<i>S. mutans</i> / <i>A. viscosus</i> / <i>L. acidophilus</i>)	Sim	VIP/FC value of each contrast group		
				sw-kb	pt-kb	zs-kb
1 Xylitol	0.990/0.998/0.953	0.031/0.001/0.025	812	1.27/4.61	1.18/3.75	1.27/2.45
2 Xylose	0.873/0.984/0.992	0.043/0.005/0.002	910	1.10/2.81	1.18/1.77	1.02/1.86
3 Phenylacetic acid	0.996/0.905/0.931	0.001/0.008/0.007	868	1.27/26.33	1.24/25.76	1.33/4.46
4 Phenyllactic acid	0.907/0.968/0.995	0.008/0.011/0.002	579	1.27/4.11	1.11/1.93	1.17/1.48
5 Phenylpyruvate	0.990/0.994/0.948	0.003/0.002/0.017	852	1.28/25.10	1.35/23.51	1.36/22.20
6 Glutaraldehyde	0.869/0.949/0.983	0.288/0.355/0.446	430	1.08/6.60	1.16/5.62	1.23/4.47
7 L-tryptophan	0.990/0.806/0.724	0.003/0.037/0.016	868	1.27/12.15	1.33/7.05	1.32/2.31
8 L-glutamic acid	0.996/0.932/0.903	0.003/0.042/0.041	435	1.03/24.08	1.12/6.76	1.03/2.82
9 L-tyrosine	0.982/0.911/0.993	0.005/0.008/0.006	755	1.28/7.09	1.05/2.93	1.18/2.13
10 Xanthine	0.995/0.835/0.752	0.002/0.025/0.008	825	1.27/8.68	1.30/3.84	1.17/1.91

Table 2. Metabolites at the sw phase related to the diameter of inhibitory ring

Metabolites	<i>r</i> (<i>S. mutans</i> / <i>A. viscosus</i> / <i>L. acidophilus</i>)	<i>P</i> (<i>S. mutans</i> / <i>A. viscosus</i> / <i>L. acidophilus</i>)	Sim	VIP/FC value sw-others
1 Tartronic acid	0.990/0.906/0.900	0.003/0.006/0.023	494	2.06/-
2 Glycolic acid	0.990/0.963/0.980	0.003/0.012/0.007	805	1.73/-
3 L-Malic acid	0.990/0.905/0.902	0.003/0.006/0.002	471	1.73/-
4 D-Tagatose	0.990/0.806/0.702	0.003/0.030/0.039	309	1.73/-
5 Spermidine	0.996/0.861/0.776	0.001/0.042/0.027	886	1.72/-

Notes: In **Tables 1** and **2**, *r* refers to the correlation coefficient; *P* refers to the hypothesis test value of correlation coefficient; sim refers to the similarity; VIP refers to the variable importance in the projection value; FC refers to the peak area ratio of metabolites between the two groups. In the column of "sw-others", the peak area of the selected metabolite at the sw phase was much larger than that at the remaining phases.

could effectively inhibit the growth, adhesion, and acid production of *A. viscosus*. Furthermore, M kinen [23] and S Derling E [24] believed that xylitol could reduce acid production and inhibit the acid-tolerant oral flora growth, which results in the decline of the number of lactobacilli in the oral cavity. According to the discrimination analysis and antibacterial correlation analysis in our study, it was found that xylitol is significantly positively correlated with the diameter of bacteriostatic zones in *S. mutans*, *L. acidophilus*, and *A. viscosus* (*r* = 0.990, 0.998 and 0.953 respectively; *P* < 0.05). This implies that xylitol is a kind of small molecule metabolite produced by *B. subtilis* zh7 which could inhibit the growth of the three types of the cariogenic bacteria (*S. mutans*, *L. acidophilus*, and *A. viscosus*).

In our study, we found that *B. subtilis* zh78 could produce higher levels of phenyllactic acid, phenylacetic acid, and phenylpyruvate at the zs, the pt, and the sw growth phases, all of which were located in the phenylalanine metabolism pathway. Phenylacetic acid and phenyl-

lactate acid were the downstream products from phenylpyruvate. Phenyllactic acid (PLA), known as a universal antimicrobial agent, could exert inhibitory effects on a range of Gram-negative bacteria and Gram-positive bacteria and it has been used as a platelet-aggregation inhibitor in 'Danshensu' medicine in China [25]. Phenylacetic acid has previously been demonstrated to display growth-inhibitory activity towards Gram-negative bacteria, Gram-positive bacteria, and fungi [26]. It was often adopted as the side-chain precursor in the pharmaceutical industry for the penicillin G production [27]. All of the three products from *B. subtilis* zh78 were significantly positively correlated with the diameter of inhibition circle in *S. mutans*, *L. acidophilus*, and *A. viscosus*. According to their bacteriostatic mechanism and their correlation with the bacteriostatic ring, it could be deduced that phenyllactate acid and phenylacetic acid produced by *B. subtilis* zh78 were the substances with broad-spectrum antibacterial activity while phenylpyruvate could promote the antibacterial effects in phenylacetic acid and phenyllactate acid.

The glutaraldehyde and the aldehyde-based disinfectant has been widely applied as a high-level disinfectant for semi-critical and temperature-sensitive medical devices in hospitals worldwide [28]. In this study, glutaraldehyde was found in the metabolic products from *B. subtilis zh78* growth at the zs, the pt, and sw stages and its correlation with the inhibition zone was strong. This might be the reason why the antimicrobial effects of metabolites from *B. subtilis zh78* were significant.

L-glutamic acid is a white crystalline powder, with a special taste and acidity, that plays a key role in many aspects including nutritional metabolism, energy requirements, immune response, oxidative stress, signal pathway regulation, and synaptic transmission [29]. Except for being an element of protein synthesis, L-tyrosine (a kind of non-essential aromatic amino acid) also serves as a precursor to melanin pigment, catecholamines, tyramine/octopamine, and thyroid hormones [30]. In a previous study [31], *S. mutans* along with glutamic acid and the other 20 kinds of free amino acids were cultured. It was found that the D- and L- typed glutamic acid could inhibit *S. mutans* growth and its biofilm formation and the D- and L- typed tyrosine could retard *S. mutans* growth [31]. In this study, it was shown that levels of L-glutamic acid and L-tyrosine were high at the different growth stages (zs, pt, and sw) of *B. subtilis zh78* and their correlation with the diameter of the bacteriostatic ring in *S. mutans* were significant ($r = 0.990$ and 0.982 ; $P = 0.003$ and 0.006). The results indicate that L-glutamic acid and L-tyrosine, the small molecule metabolites produced by *B. subtilis zh78* during the zs, the pt, and sw growth stages, have obvious inhibitory effects on *S. mutans*. Among the antibacterial substances appearing at the zs, the pt, and the sw growth phases of *B. subtilis zh78*, L-tryptophan [32], xanthine [33], and xylose [34] showed certain antibacterial activity but their relationships with *S. mutans*, *L. acidophilus*, and *A. viscosus* were still ambiguous.

Some substances (tartronic acid, D-tagatose, L-malic acid, glycolic acid, and spermidine) were only produced at the sw growth phase of *B. subtilis zh78* and their correlations with the inhibition zones in *S. mutans*, *L. acidophilus*, and *A. viscosus* were significant (shown in **Table 2**).

L-malic acid and glycolic acid are organic acids and organic acids have been proven to possess important antimicrobial properties which have been attributed to the reduction of the medium pH, the decrease of intracellular pH, and the disruption of substrate transport [35]. Malic acid is a dicarboxylic acid that exists in the form of L-isomer [36]. L-malic acid, the main organic acid, is found in most unripe fruits and could induce fleshy fruit acidity. It was indicated by Eswaranandam [37] that malic acid had strong antimicrobial activity. It was also reported that significant bactericidal effects on some microorganisms could be observed when malic acid was added to the dipping solution [35]. Glycolic acid naturally exists in grapes, sugar cane juice, sugar beets, and Virginia creeper leaves. It intrinsically possesses antimicrobial and antifungal characteristics which have been widely applied as an agent in the office-based peels as well as in cosmetic products [38]. In this study, higher contents of glycolic acid and L-malic acid were only discovered at the sw growth stage of *B. subtilis zh78* and both of the acids were highly correlated with the diameter of the inhibition zone. Therefore, it was speculated that glycolic acid and L-malic acid produced at the sw growth period of *B. subtilis zh78* were two kinds of the small molecule metabolites with broad-spectrum antibacterial activity. Metabolites produced at the sw growth phase of *B. subtilis zh78* displayed significant inhibitory effects on cariogenic bacteria (*S. mutans*, *L. acidophilus*, and *A. viscosus*), which might be partially attributable to the antibacterial effects of L-malic acid and glycolic acid.

Previous studies have demonstrated that tartronic acid could block aerobic glycolysis due to its inhibitory effect on lactic dehydrogenase [39]. It was deduced from our study that lactic dehydrogenase was the only glycolytic enzyme which could block the glycolysis of the bacteria (*S. mutans*, *L. acidophilus*, and *A. viscosus*) and thus inhibited their growth. Since *L. acidophilus* only possessed the glycolytic pathway and lactic acid was its only metabolic product, the inhibitory effects of tartronic acid on *L. acidophilus* would be much stronger.

D-tagatose, a rare monosaccharide, is a differential isomer of fructose. It is similar to the xylitol and the other polyols which could pro-

duce less acid and would not reduce the pH value in the oral cavity, thus effectively preventing enamel demineralization. Therefore, it could exert anticaries effects [40]. This study shows that the content of D-tagatose was significantly higher at the sw growth stage of *B. subtilis zh78*, which had a strong correlation with the diameter of the inhibition zone. The data suggests that D-tagatose could inhibit growth of cariogenic bacteria (*S. mutans*, *L. acidophilus*, and *A. viscosus*) and could prevent dental caries. Furthermore, spermidine also had certain antibacterial effects [41]. Its relationship with cariogenic bacteria (*S. mutans*, *L. acidophilus*, and *A. viscosus*) is still ambiguous and needs to be explored further in future studies.

In summary, among the small molecular metabolites produced by *B. subtilis zh78*, antibacterial substances including xylitol, L-glutamic acid, and L-tyrosine could inhibit the growth of *S. mutans* and other cariogenic bacteria. This study provides theoretical basis for the application of *B. subtilis zh78* to prevent dental caries in the future. The probiotic role of *B. subtilis zh78* should be explored in further studies.

Acknowledgements

This study was financially supported by the Area Fund Projects of the Chinese National Natural Science Funds (31560159, 31760159, /C0309), the National Natural Science Foundation of China (81773942), the Science and Technology Support Project in Gansu Province (17JR5RA274), and the Key Colleges and Universities Focus on Nurturing Projects (319-20170162). This study was fully sponsored by Gansu GeneBioYea Biotech Co. Ltd. The funders had no role in study design, data collection and interpretation, or the decision to submit the work for publication.

Disclosure of conflict of interest

None.

Address correspondence to: Jianye Zhou, Zhiqiang Li, Key Laboratory of Oral Diseases, Key Lab of Stomatology of State Ethnic Affairs Commission, 1 Northwest Village, Lanzhou, Gansu Province, China. Tel: 0086-931-2738557; Fax: 0086-931-2738557; E-mail: 14092785@qq.com (ZJY); lizhiqiang6767@163.com (LZQ)

References

- [1] Xin Z, He J, Lin W, Zhou S, Xian P, Shi H, Zheng L, Lei C, Hao Y and Li J. Ecological effect of arginine on oral microbiota. *Sci Rep* 2017; 7: 7206.
- [2] Cura F, Palmieri A, Girardi A, Martinelli M, Scapoli L and Carinci F. Lab-Test® 4: Dental caries and bacteriological analysis. *Dent Res J* 2012; 9: 139-141.
- [3] Chen J, Li T, Zhou X, Cheng L, Huo Y, Zou J and Li Y. Characterization of the clustered regularly interspaced short palindromic repeats sites in *Streptococcus mutans* isolated from early childhood caries patients. *Arch Oral Biol* 2017; 83: 174-180.
- [4] Byun R, Nadkarni MA, Chhour KL, Martin FE, Jacques NA and Hunter N. Quantitative analysis of diverse *Lactobacillus* species present in advanced dental caries. *J Clin Microbiol* 2004; 42: 3128-3136.
- [5] Tao R, Tong Z, Lin Y, Xue Y, Wang W, Kuang R, Wang P, Tian Y and Ni L. Antimicrobial and antibiofilm activity of pleurocidin against cariogenic microorganisms. *Peptides* 2011; 32: 1748-1754.
- [6] Zhang Q, Nijampatnam B, Hua Z, Nguyen T, Zou J, Cai X, Michalek SM, Velu SE and Wu H. Structure-based discovery of small molecule inhibitors of cariogenic virulence. *Sci Rep* 2017; 7: 5974.
- [7] Tahmourespour A and Kermanshahi RK. The effect of a probiotic strain (*Lactobacillus acidophilus*) on the plaque formation of oral *Streptococci*. *Bosn J Basic Med Sci* 2011; 11: 37-40.
- [8] Poormontaseri M, Hosseinzadeh S, Shekarforoush SS and Kalantari T. The effects of probiotic *Bacillus subtilis* on the cytotoxicity of *Clostridium perfringens* type a in Caco-2 cell culture. *BMC Microbiol* 2017; 17: 150.
- [9] Tahir HAS, Gu Q, Wu H, Raza W, Safdar A, Huang Z, Rajer FU and Gao X. Effect of volatile compounds produced by *Ralstonia solanacearum* on plant growth promoting and systemic resistance inducing potential of *Bacillus* volatiles. *BMC Plant Biol* 2017; 17: 133.
- [10] Naidorf IJ. Clinical microbiology in endodontics. *Dent Clin North Am* 1974; 18: 329-344.
- [11] Sunde PT, Olsen I, Lind PO and Tronstad L. Extraradicular infection: a methodological study. *Endod Dent Traumatol* 2000; 16: 84-90.
- [12] Yamane K, Ogawa K, Yoshida M, Hayashi H, Nakamura T, Yamanaka T, Tamaki T, Hojoh H, Leung KP and Fukushima H. Identification and characterization of clinically isolated biofilm-forming gram-positive rods from teeth associated with persistent apical periodontitis. *J Endodont* 2009; 35: 347-352.

- [13] You XL, Wang SG, Zeng SA, Zhou JY, Wang JJ, Che CX, Li ZQ and He XY. In vitro inhibitive activity of *Bacillus subtilis* isolated from oral cavity. *J Oral Sci Res* 2015; 31: 991-994.
- [14] Patti GJ, Yanes O and Siuzdak G. Metabolomics: the apogee of the omic trilogy. *Nat Rev Mol Cell Bio* 2013; 13: 263-269.
- [15] Cocco F, Carta G, Cagetti MG, Strohmenger L, Lingström P and Campus G. The caries preventive effect of 1-year use of low-dose xylitol chewing gum. A randomized placebo-controlled clinical trial in high-caries-risk adults. *Clin Oral Investig* 2017; 21: 2733-2740.
- [16] Beenken KE, Bradney L, Bellamy W, Skinner RA, McLaren SG, Gruenwald MJ, Spencer HJ, Smith JK, Haggard WO and Smeltzer MS. Use of xylitol to enhance the therapeutic efficacy of polymethylmethacrylate-based antibiotic therapy in treatment of chronic osteomyelitis. *Antimicrob Agents Chemother* 2012; 56: 5839-5844.
- [17] Reiner AM. Xylitol and D-arabitol toxicities due to derepressed fructose, galactitol, and sorbitol phosphotransferases of *Escherichia coli*. *J Bacteriol* 1977; 132: 166-173.
- [18] Hrimech M, Mayrand D, Grenier D and Trahan L. Xylitol disturbs protein synthesis, including the expression of HSP-70 and HSP-60, in *Streptococcus mutans*. *Oral Microbiol Immun* 2000; 15: 249-257.
- [19] Söderling EM and Hietalalenkkeri AM. Xylitol and erythritol decrease adherence of polysaccharide-producing oral streptococci. *Current Microbiology* 2010; 60: 25-29.
- [20] Ly KA, Milgrom P, Roberts MC, Yamaguchi DK, Rothen M and Mueller G. Linear response of *Streptococcus mutans* to increasing frequency of xylitol chewing gum use: a randomized controlled trial. *BMC Oral Health* 2006; 6: 6.
- [21] Houzuo G, Yao X, Xiaotian L and Ling Z. [In vitro study of xylitol on the growth and acid production of *Actinomyces viscosus*]. *Hua Xi Kou Qiang Yi Xue Za Zhi* 2014; 32: 217-220.
- [22] Thabuis C, Cheng CY, Wang X, Pochat M, Han A, Miller L, Wils D and Guerinderemaux L. Effects of maltitol and xylitol chewing-gums on parameters involved in dental caries development. *Eur J Paediatr Dent* 2013; 14: 303-308.
- [23] Mäkinen KK, Alanen P, Isokangas P, Isotupa K, Söderling E, Mäkinen PL, Wang W, Wang W, Chen X and Wei Y. Thirty-nine-month xylitol chewing-gum programme in initially 8-year-old school children: a feasibility study focusing on *Streptococcus mutans* and *Lactobacilli*. *Int Dent J* 2008; 58: 41-50.
- [24] Söderling E, Hirvonen A, Karjalainen S, Fontana M, Catt D and Seppä L. The effect of xylitol on the composition of the oral flora: a pilot study. *Eur J Dent* 2011; 5: 24-31.
- [25] Li L, Shin SY, Lee KW and Han NS. Production of natural antimicrobial compound d-phenyllactic acid using *Leuconostoc mesenteroides* ATCC 8293 whole cells involving highly active d-lactate dehydrogenase. *Lett Appl Microbiol* 2014; 59: 404-411.
- [26] Somers E, Ptacek D, Gysegom P, Srinivasan M and Vanderleyden J. *Azospirillum brasilense* produces the auxin-like phenylacetic acid by using the key enzyme for indole-3-acetic acid biosynthesis. *Appl Environ Microbiol* 2005; 71: 1803-1810.
- [27] Harris DM, van der Krogt ZA, Klaassen P, Raamsdonk LM, Hage S, van den Berg MA, Bovenberg RA, Pronk JT, Daran JM. Exploring and dissecting genome-wide gene expression responses of *Penicillium chrysogenum* to phenylacetic acid consumption and penicillinG production. *BMC Genomics* 2009; 10: 75.
- [28] De Groote MA, Gibbs S, de Moura VC, Burgess W, Richardson K, Kasperbauer S, Madinger N, Jackson M. Analysis of a panel of rapidly growing mycobacteria for resistance to aldehyde-based disinfectants. *Am J Infect Control* 2014; 42: 932-934.
- [29] Brosnan JT and Brosnan ME. Glutamate: a truly functional amino acid. *Amino Acids* 2013; 45: 413-418.
- [30] Slominski A, Zmijewski MA and Pawelek J. L-tyrosine and L-dihydroxyphenylalanine as hormone-like regulators of melanocyte functions. *Pigment Cell Melanoma Res* 2012; 25: 14-27.
- [31] Zhang LD, Ling JQ and Tong ZC. Effects of free amino acids on *Streptococcus mutans* proliferation and biofilm formation. *Chin J Conserv Dent* 2014; 24: 313-316.
- [32] Narui K, Noguchi N, Saito A, Kakimi K, Motomura N, Kubo K, Takamoto S and Sasatsu M. Anti-infectious activity of tryptophan metabolites in the L-tryptophan-L-kynurenine pathway. *Biol Pharm Bull* 2009; 32: 41-44.
- [33] Naftalin CM, Verma R, Gurumurthy M, Lu Q, Zimmerman M, Yeo BCM, Tan KH, Lin W, Yu B and Dartois V. Co-administration of allopurinol to increase anti-mycobacterial efficacy of pyrazinamide: evaluation in a whole-blood bactericidal activity model. *Antimicrob Agents Chemother* 2017; 61.
- [34] Badwaik VD, Willis CB, Pender DS, Rammohan P, Monic S, Kherde YA, Vangala LM, Gonzalez MS and Rajalingam D. Antibacterial gold nanoparticles-biomass assisted synthesis and characterization. *J Biomed Nanotechnol* 2013; 9: 1716-1723.
- [35] Raybaudi-Massilia RM, Mosqueda-Melgar J, Sobrino-López A, Soliva-Fortuny R and Martín-Belloso O. Use of malic acid and other quality stabilizing compounds to assure the safety of fresh-cut "fuji" apples by inactivation of *Listeria*

Microbial metabolomics

- monocytogenes, salmonella enteritidis and escherichia coli o157:h7. *J Food Safety* 2009; 29: 236-252.
- [36] Gou L, Zhan Y, Lee J, Li X, Lü ZR, Zhou HM, Lu H, Wang XY, Park YD and Yang JM. Effects of L-malic acid on alpha-glucosidase: inhibition kinetics and computational molecular dynamics simulations. *Appl Biochem Biotechnol* 2015; 175: 2232-2245.
- [37] Eswaranandam S, Hettiarachchy NS and Johnson MG. Antimicrobial activity of citric, lactic, malic, or tartaric acids and nisin-incorporated Soy protein film against listeria monocytogenes, escherichia coli O157:H7, and salmonella gaminara. *J Food Sci* 2010; 69: FMS79-84.
- [38] Abels C, Kaszuba A, Michalak I, Werdier D, Knie U, Kaszuba A. A 10% glycolic acid containing oil-in-water emulsion improves mild acne: a randomized double-blind placebo-controlled trial. *J Cosmet Dermatol* 2011; 10: 202-209.
- [39] Fiume L, Manerba M, Vettraino M and Stefano GD. Impairment of aerobic glycolysis by inhibitors of lactic dehydrogenase hinders the growth of human hepatocellular carcinoma cell lines. *Pharmacology* 2010; 86: 157-162.
- [40] Wong D. Sweetener determined safe in drugs, mouthwashes, and toothpastes. *Dent Today* 2000; 19: 32, 34-35.
- [41] Sobe RC, Bond WG, Wotanis CK, Zayner JP, Burriss MA, Fernandez N, Bruger EL, Waters CM, Neufeld HS and Karatan E. Spermine inhibits vibrio cholerae biofilm formation through the NspS-MbaA polyamine signaling system. *J Biol Chem* 2017; 292: 17025-17036.

Microbial metabolomics

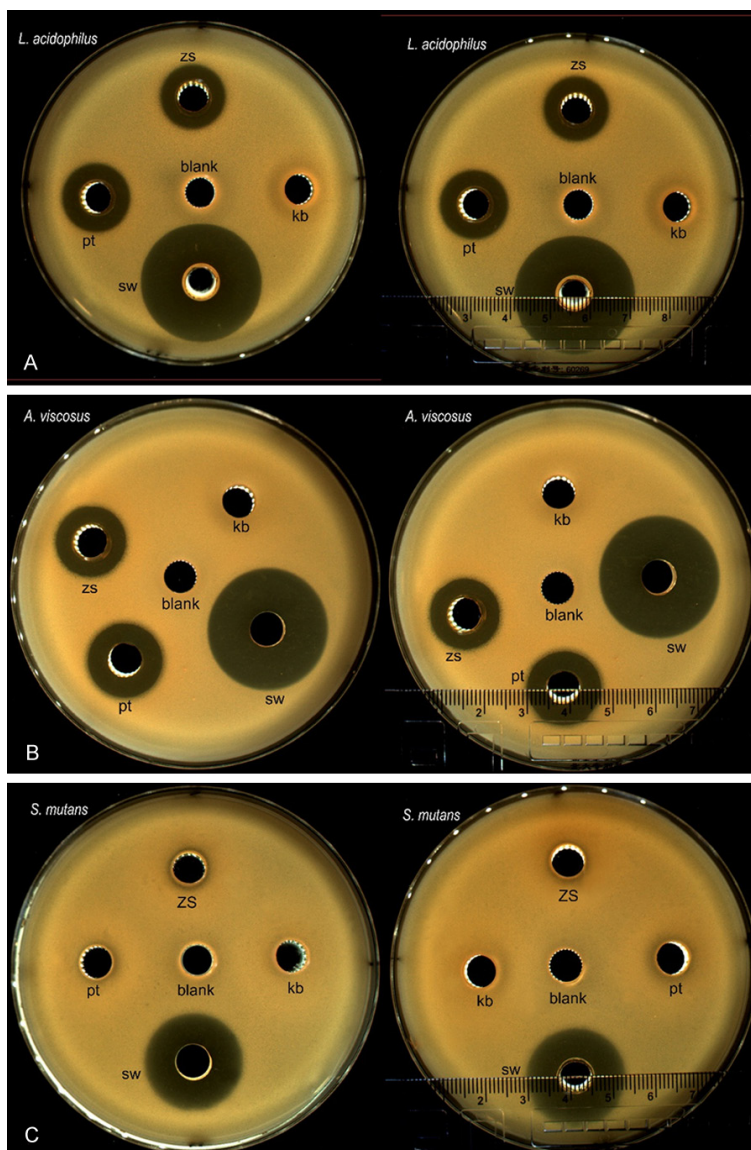


Figure S1. Inhibitory effect of metabolites of *Bacillus subtilis* at different growth stages on *L. acidophilus* (A), *A. viscosus* (B), *S. mutans* (C). Finger legends: In the culture dish of *S. mutans*, the diameters of bacteriostatic rings in were 0.85 mm-zs, 1.35 mm-pt, 14.2mm-sw; In the culture dish of *A. viscosus*, 4.1 mm-zs, 6.9 mm-pt, 18.35 mm-sw; In the culture dish of *L. acidophilus*, 7.35 mm-zs, 8.45 mm-pt, 21.05mm-sw.

Microbial metabolomics

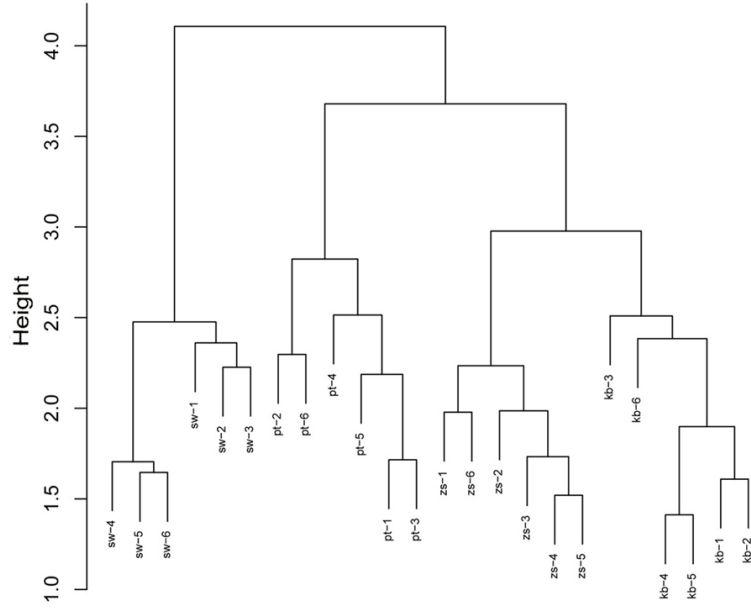


Figure S2. Cluster analysis of metabolites in kb, zs, pt and sw phases of *B. subtilis* zh78.